



Microlasers Made Entirely from Edible Substances

Abdur Rehman Anwar, Maruša Mur, Georgia Michailidou, Dimitrios N. Bikiaris, and Matjaž Humar*

Biolasers composed of biological and biocompatible materials are increasingly used in biomedical applications, including cell barcoding and biosensing. However, no studies have focused on creating lasers from edible substances. Here, consumable substances for both the laser cavity and the gain material are systematically explored. Several fluorescent dyes are identified as effective gain materials for lasing. Two types of microcavities are demonstrated: whispering gallery mode and Fabry-Pérot. The edible microlasers are employed as sensors and barcodes. Due to their extremely narrow spectral lines, the microlasers provide exceptional sensitivity to various environmental factors. They are designed to sense sugar concentration, pH, the growth of bacteria, and exposure to too-high temperatures. Additionally, they encode multiple data bits, such as manufacturer information and expiration dates, while also functioning as physical unclonable functions for anti-counterfeiting. The microlasers developed in this study are entirely safe for consumption, do not alter the appearance or taste of food, and are environmentally friendly. Unlike traditional barcodes and sensors placed on the packaging, edible lasers can be embedded directly into edible products. They can significantly enhance traceability, security, and freshness monitoring of food and pharmaceuticals as well as non-edible products and can be employed for environmental monitoring and biomedical applications.

A. R. Anwar, M. Mur, M. Humar Department of Condensed Matter Physics J. Stefan Institute Jamova 39, Ljubljana SI-1000, Slovenia E-mail: matjaz.humar@ijs.si

A. R. Anwar

Jožef Stefan International Postgraduate School Jamova 39, Ljubljana SI-1000, Slovenia

G. Michailidou, D. N. Bikiaris

Laboratory of Polymer Chemistry and Technology, Department of

Aristotle University of Thessaloniki Thessaloniki GR-54124, Greece

M. Humar CENN Nanocenter

Jamova 39, Ljubljana SI-1000, Slovenia

M. Humar

Faculty of Mathematics and Physics

University of Ljubljana

Jadranska 19, Ljubljana SI-1000, Slovenia



The ORCID identification number(s) for the author(s) of this article can be found under https://doi.org/10.1002/adom.202500497

© 2025 The Author(s). Advanced Optical Materials published by Wiley-VCH GmbH. This is an open access article under the terms of the Creative Commons Attribution License, which permits use, distribution and reproduction in any medium, provided the original work is properly cited.

DOI: 10.1002/adom.202500497

1. Introduction

In recent years, biological and biomaterial microcavities and microlasers have gained much attention because of their potential in tracking, labeling, bio-detection, cell barcoding, information security, and anticounterfeiting. Microlasers have a narrow emission spectrum and, therefore, are very sensitive to environmental factors and have the potential to generate millions of unique tags. They have been increasingly employed as barcodes[1-4] and microsensors,[5-8] however, until now they have mainly been applied to biomedical applications[9] and were not made explicitly from edible materials. There are several instances where either the cavity or the gain medium, but not both, were made from bio-materials appropriate for consumption.[10-13] Only a few studies have reported microcavities made entirely from edible materials, emitting above or below the lasing threshold. However, these were not explicitly designed for consumption or use in food.[14-16]

Counterfeiting and poor quality are rising concerns in the food and pharmaceutical industry as they are directly linked to public health. There are various reliable conventional methods to evaluate food quality and authenticity, such as mass spectrometry, DNA barcoding, isotope, and elemental fingerprints, and gas chromatography.[17,18] However, these techniques require sophisticated instrumentation; they are time-consuming, expensive, inappropriate for consumer use, and usually require sample collection to be analyzed. Barcodes on the packaging are unsuitable for bulk unpackaged goods and in the case of packaged items, the packaging can be removed or substituted. An edible barcode or sensor embedded directly into the product and remotely read by a small handheld reader would be ideal for these applications. A few solutions exist^[19,20] but are either only at a proof-ofconcept stage, are only partially edible, or require complex readout methods. Monitoring food freshness, along with traceability, is crucial for safety and reducing waste, as food often remains good past its expiration date. Various sensors for active monitoring of parameters like pH and humidity have been integrated into packaging, creating smart, or intelligent packaging. [21] Edible or biodegradable sensors were reported but mostly applied to biomedical research.[22-24]

In this work, we aimed to systematically search and test different dyes, cavity materials, and geometries to make completely edible lasers and employ them for various applications related to food and pharmaceuticals for the first time (**Figure 1**).

21951071, 2025, 22, Downloaded from https://advanced.onlinelibrary.wiley.com/doi/10.1002/adom.202500497 by Matjaž Humar - Institut Jozef Stefan , Wiley Online Library on [08/08/2025]. See the Terms and Conditions (https://onlinelibrary.wiley.

and-conditions) on Wiley Online Library for rules of use; OA articles are governed by the applicable Creative Commons

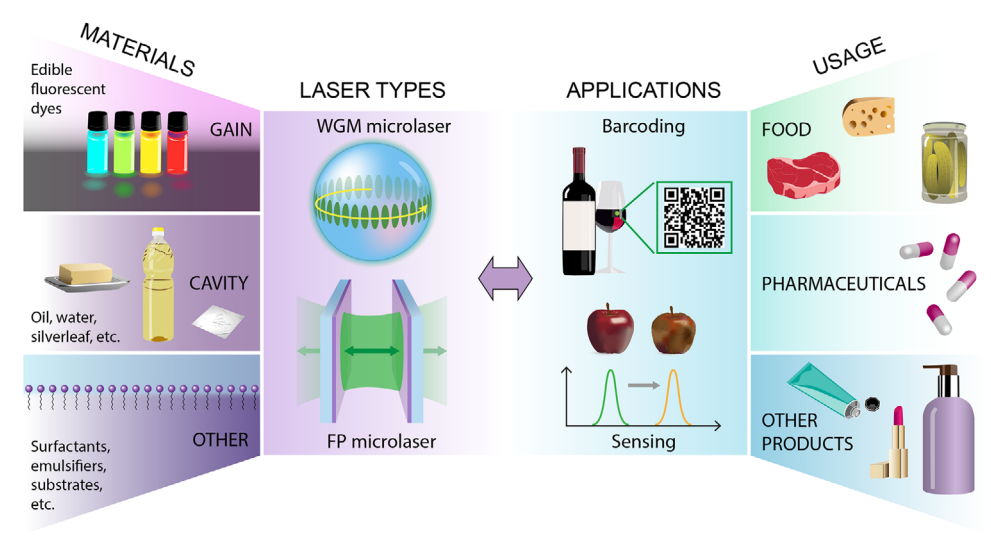


Figure 1. Development of completely edible microlasers in different configurations: from materials to applications. Various edible laser gain materials, cavity materials and optional secondary materials were identified and employed to make two types of lasers: whispering gallery mode (WGM) and Fabry-Pérot (FP) microlasers. These lasers were employed for barcoding and sensing, enhancing authentication, and reducing the health risks of various products, including food, pharmaceuticals, and non-edible products.

2. Results

2.1. Basic Concepts and Constituents of Edible Microlasers

A laser consists of three main components: a gain medium, an optical cavity, and an energy source. In our case, the gain medium is a fluorescent dye that provides optical gain through stimulated emission. Based on their light confinement mechanism, microcavities can be of different types. We demonstrated two types, whispering gallery mode (WGM) and Fabry-Pérot (FP) microlasers. The microlasers are pumped with an external light source, such as a pulsed laser. When the optical gain in the cavity exceeds the optical losses, the system reaches the lasing threshold, emitting laser light. Here, we used only edible substances for both the gain medium and the cavity, either naturally occurring in food or approved food additives, without any chemical alterations (Table 1).

Many food colorants are available, and among them, we searched for dyes with sufficiently strong fluorescence for use as the gain material. Dyes with a quantum yield below ≈0.2 were unsuitable for lasing. In some cases, dyes with sufficient quantum yield were limited by their solubility in common food solvents (e.g., water and oils). We did not consider pure ethanol as a solvent due to its impracticality, as it evaporates quickly or diffuses into surrounding food. Further, we did not consider dyes that are safe to ingest but are not approved for food use, such as fluorescein and fluorescent proteins. [9,28-33] The choice of resonator material depends on the microlaser configuration and function. Typically, these materials should be transparent and, in some configurations, need to have a high refractive index or be reflective if used as a mirror. We used various oils, butter, agar, gelatin, chitosan, and thin silver leaves to produce cavities. Additional materials were used for non-optical components, such as for mechanical support, encapsulation, or stabilizing droplet emulsions.

In general, none of the substances used were chemically modified in any way. They were used in reasonable quantities and forms, commonly present in food and pharmaceuticals. Therefore, products' visual appearance, taste, or nutritional value were not changed considerably and remained environmentally friendly.

Table 1. List of demonstrated edible lasers including dye used, pumping and central lasing wavelengths, quantum yield (QY), solvent, and laser type.

| Dye | Pumping/lasing | QY | Solvent | Laser type |
|--|-------------------|----------------------|----------------|--|
| Chlorophyll-A | 440 or 525/680 nm | 0.3[25] | sunflower oil | WGM (oil droplets in water) FP |
| | | | cooked butter | WGM (solid beads in water) |
| Chlorophyll (naturally present in olive oil) | 440 or 525/680 nm | | | WGM (oil droplets in water) |
| | | | | FP |
| Chlorophyll (extracted from spinach) | 440 or 525/680 nm | | sunflower oil | WGM (oil droplets in water) |
| Riboflavin (vitamin B ₂) | 450/550 nm | 0.27 ^[26] | water-glycerol | WGM (droplets on a superhydrophobic surface) |
| Riboflavin sodium phosphate | 450/550 nm | 0.23 ^[27] | water | FP |
| | | | water-glycerol | WGM (droplets on a superhydrophobic surface) |
| Bixin | 450/530 nm | | sunflower oil | WGM (oil droplets in water) |

21951071, 2025, 22, Downloaded from https://advanced.onlinelibrary.wiley.com/doi/10.1002/adom.202500497 by Matjaž Humar-

, Wiley Online Library on [08/08/2025]. See the Terms:

and Conditions (https://onlinelibrary.wiley.com/term/

and-conditions) on Wiley Online Library for rules of use; OA articles are governed by the applicable Creative Commons

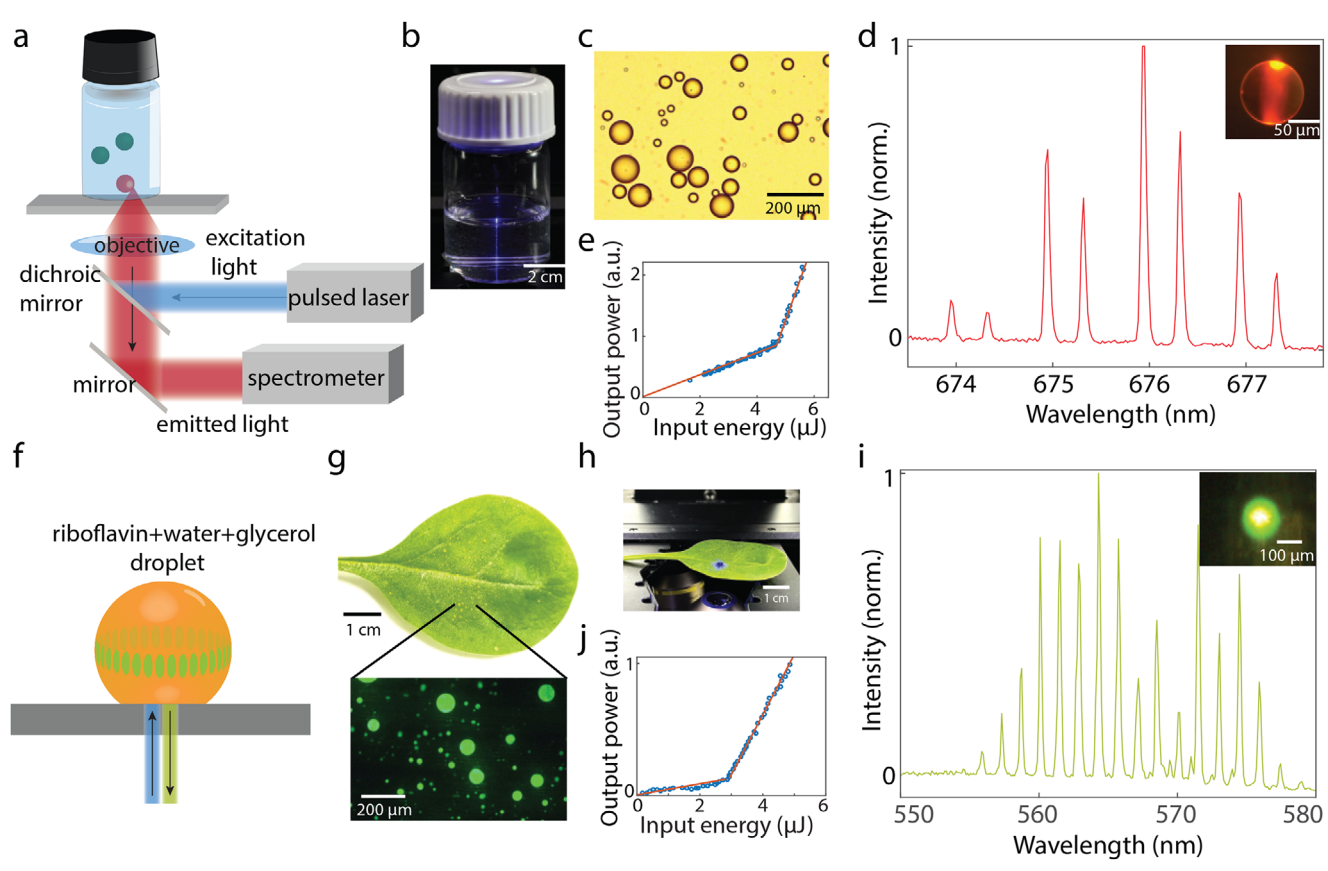


Figure 2. a) Schematics of the experimental setup, which includes a glass bottle filled with chlorophyll-doped oil droplets dispersed in water and an optical system for the excitation and signal collection. b) Chlorophyll-doped oil droplets acting as WGM lasers under the excitation of a blue pulsed laser. c) Bright-field image of polydispersed chlorophyll-doped oil droplets with a size range $20-120\,\mu\text{m}$. d) Emission spectrum (at pulse energy of $5.2\,\mu$ l) from a single chlorophyll-doped oil droplet with a diameter of approximately $100\,\mu\text{m}$ shown in the inset. e) The output power of a droplet laser (same as in d) shows a typical threshold behavior as the input pulse energy is increased. f) Scheme of an edible WGM laser as a dye-doped droplet on a superhydrophobic surface. g) Riboflavin-doped water-glycerol solution was sprayed onto a spinach leaf and the fluorescence of the resulting droplets was imaged. h) The spinach leaf was positioned on the microscope and excited by a blue pulsed laser to achieve lasing. i) Laser emission spectrum (at pulse energy of $4\,\mu$ J) from a single droplet shown in the inset. j) Output of a droplet laser (same as in i) on a leaf as the pump energy is increased shows typical threshold behavior.

2.2. Edible Whispering Gallery Mode Lasers

WGM-based microlasers are composed of dyed-doped droplets or solid spheres in a lower refractive index environment. These microcavities confine light via multiple total internal reflections on the smooth surface. WGMs typically have very high Q-factors and, therefore, low lasing thresholds. For this reason, we used WGMs to test possible candidate dyes. Specifically, oilsoluble dyes were tested in sunflower oil droplets dispersed in water (Figure 2a–c), and water-soluble dyes were tested in water droplets on a superhydrophobic surface. We achieved lasing with 2 mM chlorophyll-A or 4 mM bixin dissolved in sunflower oil. Edible emulsifier polysorbate was added to the water phase to stabilize the droplet dispersion.

The droplets were pumped with a pulsed laser and sharp spectral lines corresponding to WGM modes with transverse-electric (TE) and transverse-magnetic (TM) polarizations were observed in the emission spectrum (Figure 2d for a chlorophyll-doped droplet and Figure S1a, Supporting Information for a bixindoped droplet). For the chlorophyll-doped droplets, the measured

Q-factors exceed 9000, which is limited by the spectrometer resolution. The laser's output power as a function of input energy displays the typical threshold behavior, which indicates lasing (Figure 2e). Chlorophyll- and bixin-doped droplets had a threshold energy of $4.7\,\mu J$ and $6.8\,\mu J$, respectively. We measured the lasing threshold of chlorophyll-doped droplets with sizes ranging from 40-60 µm. The average lasing threshold was 4.5 µJ, with a standard deviation of 0.2 µJ. The minimum droplet size required to achieve lasing was approximately 35 µm. The lasing threshold for these droplets is higher compared to WGM cavities containing high quantum yield commercial laser dyes (Figure S1b, Supporting Information), but still in a usable range and well below the damage threshold, which was observed at laser pulse energies about two orders of magnitude higher (≈500 µJ). However, the bleaching of the dye due to laser exposure occurs well below the damage threshold and may impact the microlaser output more crucially. We observed stable lasing from chlorophyll-sunflower oil droplets (size 50 μm) for up to 150 consecutive pulses on average, when pumped just above the lasing threshold, whereas in principle a single pulse is sufficient to obtain the distinct laser

www.advancedsciencenews.com



www.advopticalmat.de

emission and therefore information about the droplet size. To further assess the effects of pump laser exposure, particularly on the food products, we performed calculations to estimate the temperature rise in a droplet upon pulsed laser exposure. In chlorophyll-sunflower oil droplets (40–100 $\mu m)$ the momentary temperature rise caused by exposure to a single pulse (5 μJ) is small, between 0.2 and 1 °C, and is therefore unlikely to have any significant effect on the food.

Instead of pure chlorophyll-A, a non-purified mixture of chlorophyll extracted from spinach (Figure S1c, Supporting Information) and even pure olive oil also emitted laser light from oil droplets in water, but with a lasing threshold about three times higher. Olive oil naturally contains enough chlorophyll to be used as a laser in the form of oil droplets, without adding any other substance. WGM peaks in the spectrum were also observed below the lasing threshold (Figure S1d, e, Supporting Information), using a continuous wave (CW) laser or a light-emitting diode (LED) for the excitation.

Microlasers containing edible water-soluble dyes were also made. They were in the form of water droplets deposited on a hydrophobic surface. Many plant leaves are hydrophobic/superhydrophobic (surface having a water contact angle greater than 150°).[35,36] Additionally, some edible materials can also be used to fabricate a superhydrophobic coating.[37] To test the water-soluble edible dyes, we used spinach leaves as a hydrophobic surface to make a completely edible laser (Figures 2f,g). Riboflavin and riboflavin sodium phosphate were dissolved in a water-glycerol mixture at 3 mM and 5 mM concentration, respectively. Glycerol was added to reduce the evaporation rate. The solution was sprayed onto a spinach leaf (Figure 2g), forming polydispersed microdroplets. The microdroplets emitted green fluorescent light upon excitation with a blue LED (Figure 2g). Figure 2h shows a droplet pumped with a nanosecond pulsed laser at 450 nm, narrow irregular peaks were observed in the emitted spectrum, as shown in Figure 2i (in case of riboflavin as a gain medium) and Figure S2a (Supporting Information) (in case of riboflavin sodium phosphate as a gain medium). The laser's output power as a function of input energy displays the typical threshold behavior the laser droplet is shown in inset of figure 2i), which indicates lasing (Figure 2j). Below the lasing threshold, only fluorescence was observed (Figure S2b, Supporting Information). While this is a straightforward demonstration that lasing can be achieved with edible water-soluble dyes, water droplet lasers are impractical for real-life applications, since droplets can slip from the surface, can come into contact with other materials and eventually evaporate.

2.3. Edible Fabry-Pérot Lasers

The second type of an edible laser was based on a Fabry–Pérot resonator, a linear cavity consisting of two mirrors with a gain medium between them. The most reflective edible materials are silver, gold, and aluminum. In food they are usually used in the form of extremely thin leaves, mainly as decorations for sweets and drinks. In our proposed FP edible laser, two edible mirrors, each consisting of a thin silver leaf attached to a layer of agar for structural support, were separated by an additional agar layer

acting as a spacer, but only at the cavity edges (Figure 3a,b). The space in between the mirrors was filled with 2 mM chlorophyll solution in sunflower oil or with 5 mM riboflavin sodium phosphate solution in water. One edible mirror was made intentionally shorter to enable the excitation light to enter the cavity and the resulting laser light to exit the cavity. Upon pumping the cavity filled with a chlorophyll-doped sunflower oil with a pulsed laser, above the lasing-threshold energy of 6 µJ, sharp, equally spaced peaks appeared in the emission spectrum, indicative of lasing within the FP cavity (Figure 3c,d). The average lasing threshold was 5.9 µJ, with a standard deviation of 0.2 µJ. Similarly, lasing was also achieved with a cavity filled with riboflavin sodium phosphate solution in water (see Figure S2c, Supporting Information). Using the flexible agar for mirror substrate and especially for spacers, makes the device susceptible to mechanical deformations that could impair its lasing output. This can be solved by attaching the laser to a firm food packaging or replacing the agar with other more rigid edible materials, such as shellac, silk, and natural gums.

2.4. Edible Microlaser Barcodes

The size of a WGM microcavity can be determined from its emission spectrum with a nanometer accuracy, [38,39] and can be used as a unique barcode. Most previous studies used polydispersed microlasers to generate random barcodes. [2,3,40] Here, we instead produced lasers with precisely determined sizes to encode information. [38] Using a microfluidic droplet generator chip, we generated highly monodispersed chlorophyll-doped sunflower-oil droplets (**Figure 4**a–c).

Upon excitation with a pulsed laser, the typical WGM lasing spectrum dependent on the droplet size could be observed (Figure 4d,e). Pairs of peaks were visible, corresponding to TE and TM polarizations. To measure the size of each droplet, the peak positions were fitted to the WGM solutions, [41] using the droplet size and external refractive index as a fitting parameter, while the internal refractive index was known in advance (1.458, in case of chlorophyll-doped sunflower oil, measured with a refractometer). The diameter was fitted with an absolute error of 1.2 nm. By measuring about 50 droplets, their size coefficient of variation (CV) was typically 0.2–0.4%. A change in the refractive index of the surrounding medium results in a shift of the modes; however, the fitted diameter, which encodes the barcode, will remain unchanged. Therefore, these barcodes are robust to changes in the environment.

To generate a barcode, we produced 14 different sets of monodispersed droplets, with non-overlapping sizes in the size range 39–95 μ m (Figure 5a; Table S1, Supporting Information). A total of 14 bits of information can be encoded, as each size can be present in the food sample (1) or not (0). In this way, $2^{14} = 16.384$ unique strings of binary digits can be produced. Information such as manufacturing or expiry date, country of origin, and manufacturer identification could be encoded into food and pharmaceutical products. Depending on the desired application and specifics of the particular food product, there are many options for positioning the microlasers. By using oils of different densities (or their mixtures), the lasers can either settle at the top or the bottom of the container, or they can

21951071, 2025, 22, Downloaded from https://advanced.onlinelibrary.wiley.com/doi/10.1002/adom.202500497 by Matjaž Humar - Institut Jozef Stefan , Wiley Online Library on [08:08:2025]. See the Terms

conditions) on Wiley Online Library for rules of use; OA articles are governed by the applicable Creative Commons

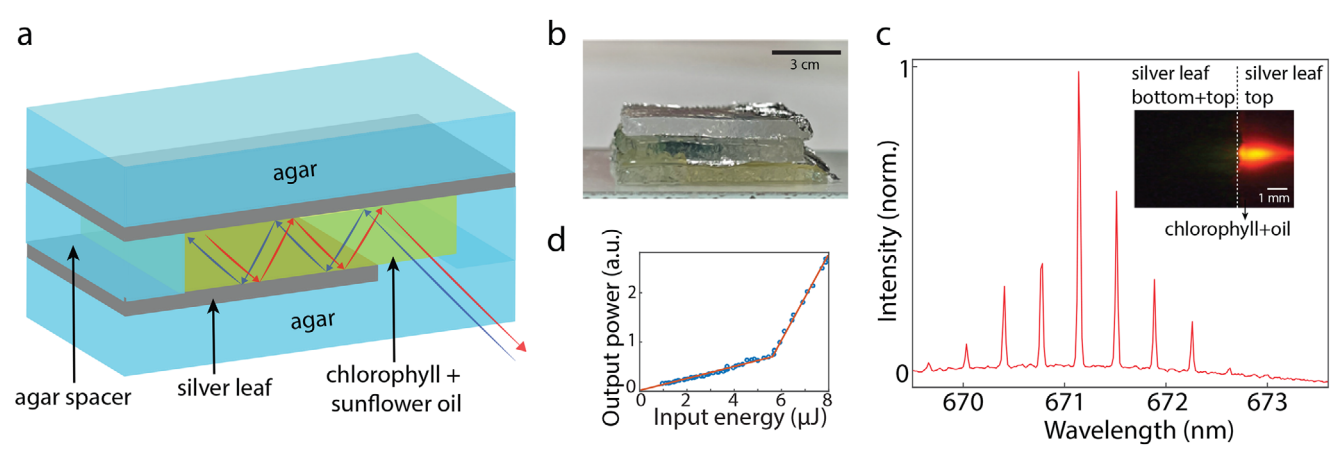


Figure 3. a) Schematics of an edible FP cavity laser. The cavity is filled with chlorophyll-doped oil and illuminated by a pulsed laser. The excitation/emission light enters/exits at the position where the silver leaf is only present on one side of the cavity. b) Side view of an edible FP cavity laser. c) Laser emission spectrum (at pulse energy of $6.5 \,\mu$ J) from an edible FP cavity shown in the inset. d) Output of a FP cavity laser (same as in (c)) as the pump energy is increased shows typical threshold behavior.

be made neutrally buoyant enabling dispersion of the microlasers throughout the whole volume of the liquid product, which is especially useful as an anti-counterfeiting measure for liquid products, e.g., olive oil and honey, which are often adulterated. For solid nontransparent food and pharmaceutical tablets, a better option would be to disperse the lasers in a matrix such as a hydrogel and spray coat it onto the surface of such products.

To demonstrate the barcoding technique we encoded a specific date into a peach compote in a glass jar and other grocery items, including a pickle jar and a juice bottle (Figure S3a,b, Supporting Information). We chose the first international "Stop Food Waste Day," commemorated on April 26, 2017. January 1, 2000 was set to be the starting day for the date encoding

scheme. This date was encoded as 0000000000001. With each unique bit-string representing one day, approximately 44 years can be covered. The first "Stop Food Waste Day" was commemorated 6325 days after the starting date of our encoding scheme. When converted into a binary string of 14 digits, 6325 equals 011000101010 (Figure 5b). In our demonstration of food expiration date encoding, we used <5 μL of sunflower oil. Each bit of encoded data contained approximately 5000 droplets. Adding 5 μL of sunflower oil to 500 mL of fruit compote increases the energy content by approximately 0.008 kcal per 100 mL, which is negligible compared to $\approx\!60$ kcal per 100 mL of fruit compote itself

To read the barcode, the glass jar was scanned with a pulsed laser (Figure 5c). When a droplet entered the illumination path,

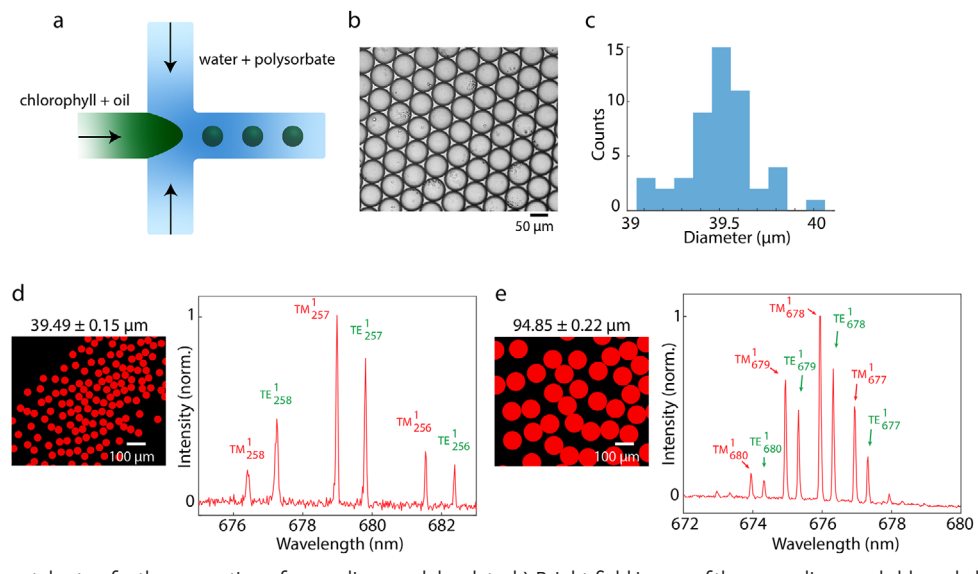


Figure 4. a) Experimental setup for the generation of monodispersed droplets. b) Bright-field image of the monodispersed chlorophyll-doped oil droplets. c) A typical size distribution of droplets within one sample. d) Fluorescence image of monodisperse chlorophyll-doped oil droplets (mean diameter $39.49 \pm 0.15 \,\mu\text{m}$) and a lasing spectrum of a single droplet. e) Fluorescence image of monodisperse chlorophyll-doped oil droplets (mean diameter $94.85 \pm 0.22 \,\mu\text{m}$) and a lasing spectrum of a single droplet.

and Conditions (https://onlinelibrary.wiley.

and-conditions) on Wiley Online Library for rules of use; OA articles are governed by the applicable Creative Commons

www.advancedsciencenews.com

www.advopticalmat.de

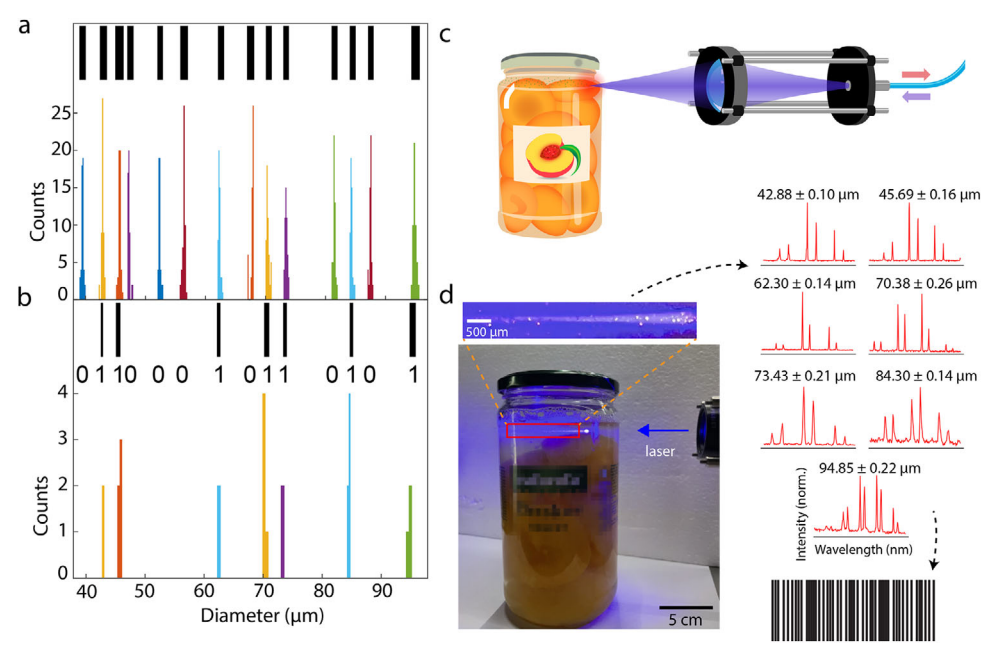


Figure 5. a) Size distribution of chlorophyll-doped oil droplets of 14 different diameters produced by a droplet generator chip. b) Distribution of droplet sizes detected in the jar after the date of "Stop Food Waste Day" was encoded by adding selected droplet sizes into the sample. All sizes were reliably detected. c) Schematics of the experimental setup for reading the barcodes, which includes an optical fiber for excitation and collection of the emission signals. d) Reading of an edible barcode based on chlorophyll-doped oil droplets in a jar of compote. The food product is scanned by a nanosecond pulsed laser at 440nm. Droplet sizes are calculated from the acquired spectra and the corresponding barcode is reconstructed.

sharp lines corresponding to WGM lasing appeared in the collected spectrum (Figure 5d). The size was calculated for each spectrum and plotted into a histogram (Figure 5b). All the sizes we inserted into the glass jar were successfully detected, with an average of five lasers of each size being detected during a few-second measurement. The barcode could be read for more than a year after it was produced by storing it at room temperature on a shelf in a glass container without any special light protection (Figure S3c, d, Supporting Information). However, beyond that period, we observed a weaker fluorescence, which was insufficient to achieve lasing. To improve the long-term stability, the lasers could be made from a solid material or embedded into an edible matrix, rather than dispersing them directly into food.

The amount of encoded information could be further increased by expanding the droplet size range, reducing size intervals, and by using higher refractive index oils such as cinnamon oil (n=1.55). In the size range 40–100 µm and a CV of 1.9 µm, in place of the 14 sizes produced on a microfluidic droplet generator chip (Figure S4a, Supporting Information), about 30 distinct sizes can be fitted without much overlap (Figure S4b, Supporting Information).

The droplet lasers can also be used as physical unclonable functions (PUFs). The small intrinsic polydispersity within each specific size range (Figure 4c) can be used to encode a random barcode, which is unique for each sample. Since the size of the oil droplet lasers can be measured down to 1 nm precision, but they can be generated only with a precision of $\approx\!200\,\mathrm{nm}$, such barcodes are unclonable. Therefore, the droplet lasers can encode some information and simultaneously be used as a PUF, providing the ultimate anti-counterfeiting measure for high-value products. If

there is no need to encode information, but only the PUF is required, then the droplets can have higher polydispersity.^[1–3] In this case, no microfluidics is necessary to generate the droplets, but instead they can be made by simply dispersing oil in water by stirring.

2.5. Sugar Concentration Measurement

Laser microcavities are highly sensitive to the changes in size, shape, and surrounding medium refractive index, which can be used to measure various parameters in food. One example is the refractive index which is typically used to determine sugar concentration in foods like wine, beer, maple syrup, and honey. A sample must be collected and inserted into a refractometer to measure the refractive index. If such a sensor was present inside the fluid itself, it would be possible to continuously monitor sugar concentration, including in a sealed container, such as in a bottle where fermentation occurs. WGM microcavities (both solid spheres and droplets) can be used to measure the absolute refractive index of the surrounding medium. [39,42] We used chlorophylldoped sunflower-oil droplets to measure the external refractive index at several different glucose concentrations. Fitting of the droplet size and the external refractive index was performed for the spectra of each droplet and the external refractive index was averaged over five droplets from each sample, with a standard deviation of 0.0003 RIU (Figure 6a). This allows a glucose concentration measurement with a 0.2 percentage point error, comparable to standard commercial refractometers. Other substances in the food apart from sugar could also change the refractive index. However, especially in the beverage industry, the refractive

21951071, 2025, 22, Downloaded from https://advanced.

Institut Jozef Stefan, Wiley Online Library on [08/08/2025]. See the Terms

and Conditions (https

and-conditions) on Wiley Online Library for rules of use; OA articles are governed by the applicable Creative Commons

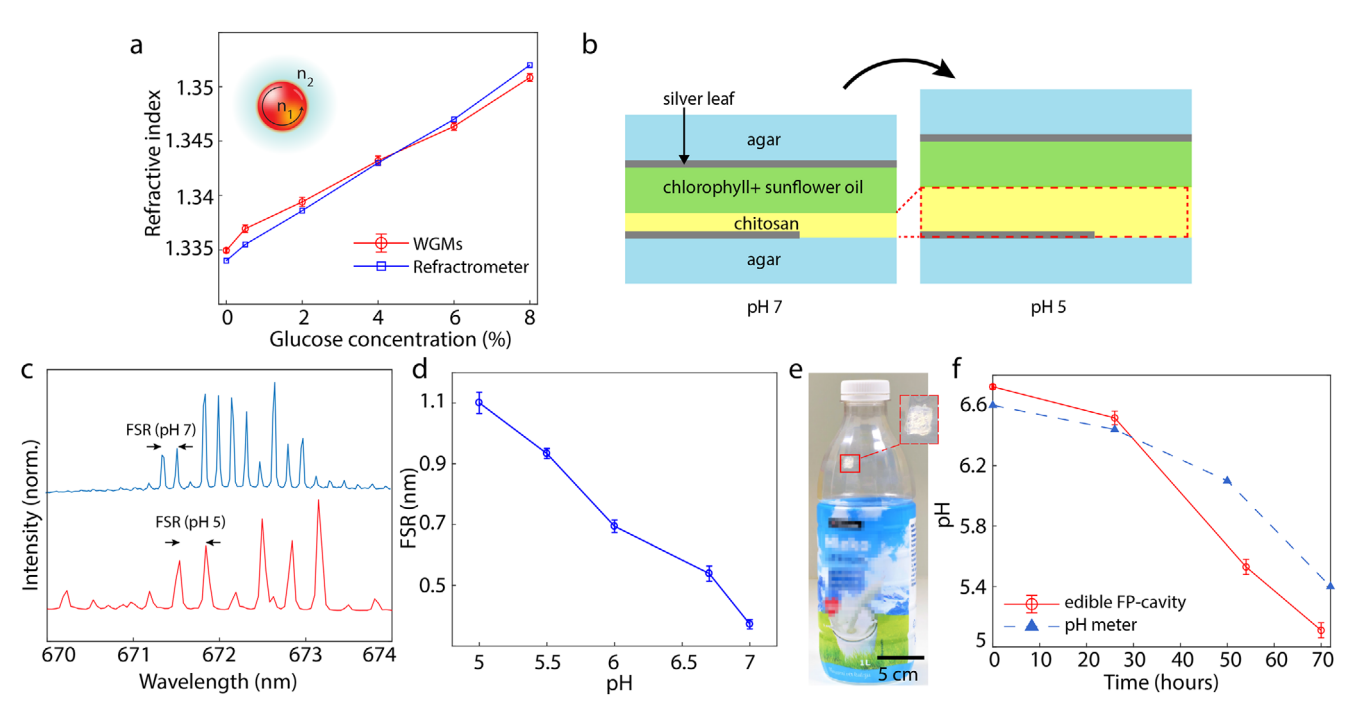


Figure 6. a) The measured refractive index of different concentrations of glucose in water. The red line is the refractive index measured via the lasing spectrum from the droplets, and the blue line are measurements performed using a refractometer. b) Schematic diagram of the edible FP cavity-based pH sensor at two different pH values. The chitosan layer swells as the pH is reduced, changing the emission of the laser. c) Emission spectra from an FP cavity pumped with a nanosecond pulsed laser at 440 nm at two different pH values. d) The change of free spectral range (FSR) with respect to the pH change. e) An edible FP-laser pH sensor inside a milk bottle measures the pH of milk. f) Change of the milk's pH over two days when left at room temperature measured by a FP laser and a pH meter on two different samples. Lowering of the pH indicates milk spoilage.

index is commonly used to measure sugar concentration. Therefore, our method is compatible with the standard measurements within these food industries.

2.6. pH Sensors

We demonstrated a completely edible pH sensor based on the edible FP cavity. The free spectral range (FSR) of a FP cavity can be calculated as $FSR = (2nL)^{-1}$, where *n* is the refractive index within the cavity and L is the cavity thickness. From the measured value of the FSR (Figure 3c), we were able to calculate the thickness of the optical cavity of 300 µm with an error of 600 nm. To make the FP microlaser pH sensitive, an additional chitosan film was introduced in between the edible mirrors (Figure 6b). Chitosan swells as the pH value decreases (Figure 5a, Supporting Information).[43] When a change in pH occurred, the thickness and refractive index of the chitosan film changed, which resulted in a change of the free spectral range of the laser emission (Figure 6c). The FSR decreased approximately linearly with increasing pH (Figure 6d). Across the sensor, the chitosan film thickness exhibited a variation of up to 0.1 mm, which translates into an error of 0.3 pH units. Therefore, to measure the pH accurately, the sensor was always pumped at the same spot, resulting in repeatable and robust measurements. The error in measuring pH was 0.05 pH units, which was estimated by repeating the measurements. In the future, if such sensors were made on an industrial scale, the thickness could easily be made much more uniform, meaning that pumping at any position would give the same result. It is worth noting that the swelling ratio changes with temperature. The swelling ratio nearly doubles at the same pH when the temperature increases from 25–45 °C.^[44] This could be compensated if temperature is measured simultaneously with another edible sensor.

We tested the pH sensor by measuring milk pH as it got spoiled over several days at room temperature. The sensor was fixed inside a milk bottle with an edible sealant (Figure 6e) and submerged in milk during the measurement. By taking into account the previously measured dependence of FSR to pH (Figure 6d), the change of pH in time was determined (Figure 6f). These results agree well with the usual drop in pH when milk gets spoiled. [45]

2.7. Detection of Microorganism Growth

We developed an FP cavity-based sensor for detecting microorganism growth inside food. The FP laser was assembled as described before (Figure 3a), except that the agar layers were replaced by nutrient-enriched gelatin (Figure 7a). During its preparation, the sensor was contaminated with microorganisms (bacteria/fungi) from air, leading to microorganism growth in gelatin in the following days. Some microorganisms produce the enzyme gelatinase, which digested the gelatin layers within several days, resulting in liquefaction of the medium. This caused the laser cavity to fall apart and not support lasing anymore (Figure 7a,b). The disappearance of the laser signal indicated

21951071, 2025, 22, Downloaded from https://advanced.onlinelibrary.wiley.com/doi/10.1002/adom.202500497 by Matjaž Humar

, Wiley Online Library on [08/08/2025]. See the Terms and Conditions (https://onlinelibrary.wiley.o

and-conditions) on Wiley Online Library for rules of use; OA articles are governed by the applicable Creative Commons I

www.advopticalmat.de

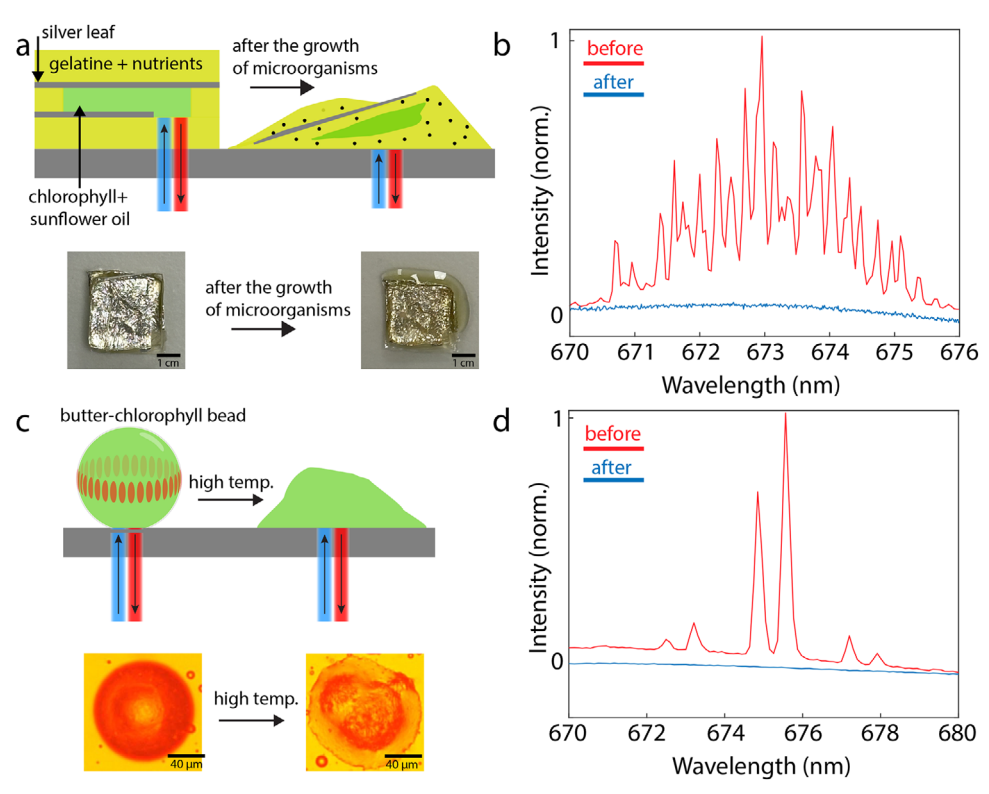


Figure 7. a) Schematic diagram of the microlaser-based microorganism sensor before and after the growth of microorganisms, and images of the microorganism sensor before (day 0) and after (day 5) the growth of bacteria (view from top). b) Emission spectra from the microorganism sensor before (day 0) and after the growth of bacteria (day 5). c) Schematic diagram of the temperature indicator before and after exposure to a high temperature, and bright-field images of the temperature sensor based on a chlorophyll-doped butter bead at low and high temperatures. d) Emission spectra from a temperature sensor at room temperature and after it has been exposed to a high temperature (35 °C).

significant microbial growth. The microbial growth is highly dependent on the temperature. Therefore, this could also indicate if the food was kept at an elevated temperature for a longer time. In some cases, mold also started growing on the sensor, which can block the light in the cavity and indicate food spoiling. Gelatin melts at elevated temperatures. This could be exploited to use it as a multifunctional sensor, not only to detect microorganism growth but also simultaneously to detect if the food was stored at a too-high temperature. Alternatively, other hydrogels less sensitive to temperature, such as agar, could be used if temperature sensitivity is undesirable. While here as a proof of concept, we purposely contaminated our sensor with microorganisms, for real-life applications, the sensor should not contain microorganisms, since this could contaminate the food. Also, the composition of the sensor must be optimized so that the rate of microorganism growth is slower than in the food product itself.

2.8. Microlaser Temperature Indicator

We developed an edible temperature indicator using a WGM laser, which irreversibly changes when exposed to a specific temperature (Figure 7c). This indicator can detect if food has been exposed to high temperature, unfrozen, or adequately heat-treated to eliminate harmful pathogens. Our indicator was made from

chlorophyll-doped butter microspheres. At a temperature above butter's melting point of 35 °C, the beads deformed, and the lasing ceased (Figure 7c,d). To show the transient change, a series of emission spectra at various temperatures is shown in the Figure S5b (Supporting Information). Once the cavity is deformed, it cannot be reversed. Therefore, it is a good indication that the temperature was above the melting point at some point during the transport or storage of food or pharmaceutical products. Our sensor can show if a product was at a temperature above the melting temperature of the sensor, but not for how long it was exposed to that temperature. Based on the desired application, cavity materials with different melting points can be used. Fatty acids have a broad range of melting temperatures from -45 to 80 °C.^[46] Edible waxes can also be used instead of fats.

3. Discussion

In this work, we demonstrated several edible lasers and their applications to enhance food and pharmaceutical security. It is the first time that edible laser dyes and microcavities were systematically studied.

Apart from WGM and FP cavities, distributed feedback (DFB) lasers and random lasers have been employed before for sensing^[47,48] and barcoding,^[49] so they could also be good candidates for the applications demonstrated here.

www.advancedsciencenews.com



www.advopticalmat.de

We searched through all the dyes allowed as food additives and tried 13 dyes that we thought had strong fluorescence (Tables S2 and 3, Supporting Information). There are possibly more edible dyes that could support lasing. For example, scopoletin and quinine have a quantum yield of $0.56^{[50]}$ and $0.58,^{[51]}$ respectively. However, they have a low solubility in common solvents. Fluorescent proteins are excellent as a laser gain material. [28,31,52] They are currently not allowed for food or pharmaceutical use. However, they are believed to pose minimal toxicity and allergenicity when ingested. [20,53]

In the current study, as a proof of concept, we employed pulsed lasers and a high-resolution spectrometer as they offer better resolution and sensitivity. However, both instruments are relatively bulky and expensive, which may not be appropriate for real-life applications. For practical use, WGM microcavities can also be operated below the lasing threshold. In this case, a CW laser or an LED source is sufficient to excite the WGM resonances. The emission spectra still show typical spectral lines. Therefore, such cavities can be used for barcoding and sensing (Figure 1d,e, Supporting Information). Additionally, compact spectrometers (pocket-sized) with sufficient spectral resolution (0.1–0.2 nm) are commercially available and are sufficient to resolve emission peaks.

This opens the possibility of using many more edible dyes, such as curcumin, $^{[16]}$ nicotinamide adenine dinucleotide (NADH), vitamin E and A_1 and porphyrins (Table S3, Supporting Information). The concepts developed within this work could also be applied to biomedical applications, where there is a wider selection of non-toxic, biocompatible, and biodegradable materials which are used for medical purposes either for ingestion, injection, or implantation.

Oil droplet-based barcodes demonstrated here are unsuitable for oil-based and solid products. Therefore, solid microspheres should be used instead. They can be produced by microfluidics from a high melting temperature fat or wax. [54,55] Parallelized microfluidic setups can generate monodispersed droplets at a high rate, making them practical for high-value products like pharmaceuticals. However, for large-scale industrial production, chemical methods to produce highly monodispersed beads [56] may be more suitable. Silica microbeads of 50 μm can be produced with a CV of 0.5 μm , sufficient to encode tens of bits of information. Silica is used in food as an anti-caking agent. [57]

Here, we demonstrated a few proof-of-concept sensors. However, microlasers enable extremely precise and sensitive detection of any physical, chemical, or biological process that changes the refractive index or physical dimension of the laser or other optical properties such as scattering, absorption and fluorescence. Therefore, many more parameters related to food safety and freshness could be measured in the future by searching for natural, or developing different responsive edible materials. The biomaterial barcodes and sensors demonstrated here could also be applied to non-edible items, such as cosmetic and agricultural products, for environmental monitoring and biomedical applications.

In conclusion, we demonstrated several edible lasers and their applications. Since this is the first such study, there are many possibilities for developing various edible lasers and their ap-

plications, which could ultimately find their way to everyday use.

4. Experimental Section

Materials: Chlorophyll-A (Sigma–Aldrich) was dissolved in ethanol and then added to sunflower oil. The ethanol was left to evaporate to yield a final dye concentration of 2 mM. Deionized water was used as a continuous phase by dissolving 1% of polyoxyethylene (20) sorbitan monolaurate (Sigma– Aldrich) as a surfactant to stabilize the droplets. Subsequently, 1% of the chlorophyll-doped sunflower oil was added into the water phase and vigorously shaken to produce droplets. Butter beads were produced in the same way just by working at a higher temperature, so the butter was liquid during the whole procedure.

Alternatively, fresh spinach leaves were used to extract the chlorophyll. They were washed with hot water and dried at $50\,^{\circ}\text{C}$ for 3-4 h. The leaves were crushed in the presence of acetone with the help of a pestle and mortar. The solution was filtered and centrifuged for $15\,\text{min}$ at $2300\,\text{g}$. Then, hexane was added to the centrifuged solution with the ratio 7(hexane):3 (centrifuged solution). The acetone and hexane formed separated layers after centrifugation (for $5\,\text{min}$ at $2300\,\text{g}$). The hexane containing chlorophyll was collected and placed on the hot plate overnight at $60\,^{\circ}\text{C}$, for the evaporation of hexane. The resulting chlorophyll was dissolved into ethanol for further use.

The FP cavity was assembled from thin silver leaves purchased at a baking supply store and agar. The agar layers were prepared by dissolving 1 g of agar (Sigma–Aldrich) in 100 g of water. The solution was sterilized by autoclaving at 121 °C for 20 min, cooled down to 65 °C and poured into plates to obtain approximately 1 mm thick films. The chitosan layer was prepared by dissolving 1 wt.% of chitosan powder (low molecular weight, Sigma–Aldrich) in 40 ml DI water that contained 2 wt.% acetic acid. This solution was poured into a silicon mold and placed in the oven for 12 h at 50 °C for the evaporation of water and acetic acid. The film was detached from the silicon mold, cut into the required sizes and washed with an ethanol solution. The final thickness of the chitosan film was in the range of 0.2–0.5 mm.

For the sensors for the detection of microorganism growth, 12% gelatine (Sigma–Aldrich) with $5\,\mathrm{gL^{-1}}$ casein hydrolysate (Sigma–Aldrich) and $3\,\mathrm{gL^{-1}}$ yeast extract (Biolife) was prepared. The mixture was sterilized by autoclaving at $121\,\mathrm{^{\circ}C}$ for $20\,\mathrm{min}$, cooled down to $65\,\mathrm{^{\circ}C}$ and poured into plates to obtain approximately $1\,\mathrm{mm}$ thick films.

The edible sealant was prepared by mixing 2.5% w/w of agar, 3.75% w/w of glycerol, and 93.75% w/w of water. The solution was placed on a hot plate at $80\,^{\circ}$ C and continuously stirred until a homogenized solution was obtained. The solution was applied to the FP cavity as a sealant.

Droplet Generation: The hydrophilized droplet generator (Fluidic 440, Chipshop) was used to produce highly monodisperse chlorophyll-doped oil droplets. The chip comprised eight different single cross channels (flow focusing geometry) with nozzle sizes 50–80 μm . Each channel contained two inlets for the oil and water phase and one outlet for the collection of droplets. Elveflow OB1 pressure controller was used to control the pressure at both inlets precisely. Droplets of 95 μm diameter were produced by using a single cross channel with a nozzle size of 80 μm by setting the pressure to 60 mbar at the chlorophyll-doped oil inlet and 25 mbar at the water-surfactant inlet. By varying the pressure at one or both inlets and using additional channels with different nozzle sizes, 14 different sizes/samples of monodispersed chlorophyll-doped oil droplets were produced.

Optical Setup: The samples were observed with an inverted microscope (Nikon Ti2) through a 20 \times /0.45 NA objective. To attain lasing, a tunable nanosecond pulsed laser (Opotek, Opolette 355) at a repetition rate of 20 Hz was used. The pump wavelength was chosen near the maximum absorption of each dye (Table 1). The spot size of the pump laser beam was approximately 30 μm , which was smaller than the diameter of the WGM lasers. The resulting fluorescent light or lasing signals were

21951071, 2025, 22, Downloaded from https://advanced.

onlinelibrary wiley.com/doi/10.1002/adom.202500497 by Matjaž Humar - Institut Jozef Stefan , Wiley Online Library on [08/08/2025]. See the Terms

and Conditions

and-conditions) on Wiley Online Library for rules of use; OA articles are governed by the applicable Creative Common



captured by a high-resolution spectrometer (Andor Shamrock SR-500i, Newton) and a digital camera (Andor Zyla) was used for imaging.

Supporting Information

Supporting Information is available from the Wiley Online Library or from the author.

Acknowledgements

This project has received funding from the European Research Council (ERC) under the European Union's Horizon 2020 research and innovation programme (grant agreement No. 851143 and 101188166), from the European Union's Horizon 2020 research and innovation programme under the Marie Sklodowska-Curie (grant agreement No. 956265), from Human Frontier Science Program (RGY0068/2020) and from the Slovenian Research And Innovation Agency (ARIS) (P1-0099 and N1-0362). The authors thank Ana Krišelj for the help in preparing the samples and Rok Štanc and Uroš Tkalec for the help with the initial experiments with microfluidics.

Conflict of Interest

The authors declare no conflict of interest.

Author Contributions

A.R.A. performed most experimental work and analysis of the results. M.M. performed some of the initial experiments and analysis. G.M. and D.N.B. provided the chitosan samples. M.H. conceived the original idea and designed and supervised the study. A.R.A., M.M., and M.H. wrote the manuscript. All authors approved the final version of the paper.

Data Availability Statement

The data that support the findings of this study are available from the corresponding author upon reasonable request.

Keywords

anti-counterfeiting, barcoding, edible materials, microlasers, sensing

Received: February 13, 2025 Revised: April 24, 2025 Published online: June 4, 2025

- [1] M. Schubert, A. Steude, P. Liehm, N. M. Kronenberg, M. Karl, E. C. Campbell, S. J. Powis, M. C. Gather, Nano Lett. 2015, 15, 5647.
- [2] M. Humar, S. H. Yun, Nat. Photonics 2015, 9, 572.
- [3] N. Martino, S. J. Kwok, A. C. Liapis, S. Forward, H. Jang, H.-M. Kim, S. J. Wu, J. Wu, P. H. Dannenberg, S.-J. Jang, Y.-H. Lee, S.-H. Yun, Nat. Photonics 2019, 13, 720.
- [4] A. R. Anwar, M. Mur, M. Humar, ACS photonics 2023, 10, 1202.
- [5] D. Yu, M. Humar, K. Meserve, R. C. Bailey, S. N. Chormaic, F. Vollmer, Nat. Rev. Methods Primers 2021, 1, 83.
- N. Toropov, G. Cabello, M. P. Serrano, R. R. Gutha, M. Rafti, F. Vollmer, Light Sci. Appl. 2021, 10, 42.

- [7] Y. Wang, S. Zeng, G. Humbert, H.-P. Ho, Laser Photonics Rev. 2020, 14, 2000135.
- [8] M. Schubert, L. Woolfson, I. R. Barnard, A. M. Dorward, B. Casement, A. Morton, G. B. Robertson, P. L. Appleton, G. B. Miles, C. S. Tucker, S. J. Pitt, M. C. Gather, Nat. Photonics 2020, 14, 452.
- [9] Y.-C. Chen, X. Fan, Adv. Opt. Mater. 2019, 7, 1900377.
- [10] T. Van Nguyen, H. H. Mai, T. Van Nguyen, D. C. Duong, V. D. Ta, J. Phys. D: Appl. Phys. 2020, 53, 445104.
- [11] T. Van Nguyen, N. Van Pham, H. H. Mai, D. C. Duong, H. H. Le, R. Sapienza, V.-D. Ta, Soft Matter 2019, 15, 9721.
- [12] Y.-C. Chen, Q. Chen, X. Fan, Lab Chip 2016, 16, 2228.
- [13] S. Nizamoglu, M. C. Gather, S. H. Yun, Adv. Mater 2013, 25, 5943.
- [14] W.-J. Lin, Y.-M. Liao, H.-Y. Lin, G. Haider, S.-Y. Lin, W.-C. Liao, R.-T. Wei, P. Perumal, T.-Y. Chang, C.-Y. Tseng, Y.-S. Lo, H.-M. Lin, T.-W. Shih, J.-S. Hwang, T.-Y. Lin, Y.-F. Chen, Org. Electron. 2018, 62, 209.
- [15] Y. Choi, H. Jeon, S. Kim, Lab Chip 2015, 15, 642.
- [16] D. Venkatakrishnarao, M. A. Mohiddon, R. Chandrasekar, Adv. Opt. Mater. 2016, 5, 1600613.
- [17] S. Medina, R. Perestrelo, P. Silva, J. A. Pereira, J. S. Câmara, Trends Food Sci. Technol. 2019, 85, 163.
- [18] S. A. Wadood, G. Boli, Z. Xiaowen, I. Hussain, W. Yimin, Microchem. J. 2020, 152, 104295.
- [19] A. Esidir, N. Kayaci, N. B. Kiremitler, M. Kalay, F. Sahin, G. Sezer, M. Kaya, M. S. Onses, ACS Appl. Mater. Interfaces 2023, 15, 41373
- [20] J. W. Leem, M. S. Kim, S. H. Choi, S.-R. Kim, S.-W. Kim, Y. M. Song, R. J. Young, Y. L. Kim, Nat. Commun. 2020, 11, 328.
- [21] H. Yousefi, H.-M. Su, S. M. Imani, K. Alkhaldi, C. D. M. Filipe, T. F. Didar, ACS Sens. 2019, 4, 808.
- [22] Q. Chen, Y. Liu, K. Gu, J. Yao, Z. Shao, X. Chen, Biomacromolecules 2022, 23, 3928,
- [23] J. Kim, I. Jeerapan, B. Ciui, M. C. Hartel, A. Martin, J. Wang, Adv. healthc. mater. 2017, 6, 1700770.
- [24] I. K. Ilic, L. Lamanna, D. Cortecchia, P. Cataldi, A. Luzio, M. Caironi, ACS Sens. 2022, 7, 2995.
- [25] D. Leupold, A. Struck, H. Stiel, K. Teuchner, S. Oberländer, H. Scheer, Chem. Phys. Lett. 1990, 170, 478.
- [26] P. Drössler, W. Holzer, A. Penzkofer, P. Hegemann, Chem. Phys. 2002, 282, 429
- [27] W. Holzer, J. Shirdel, P. Zirak, A. Penzkofer, P. Hegemann, R. Deutzmann, E. Hochmuth, Chem. Phys. 2005, 308, 69.
- [28] M. C. Gather, S. H. Yun, Nat. Commun. 2014, 5, 5722.
- [29] M. C. Gather, S. H. Yun, Nat. Photonics 2011, 5, 406.
- [30] V. D. Ta, S. Caixeiro, F. M. Fernandes, R. Sapienza, Adv. Opt. Mater. **2017**, 5, 1601022.
- [31] A. Jonáš, M. Aas, Y. Karadag, S. Manioğlu, S. Anand, D. McGloin, H. Bayraktar, A. Kiraz, Lab Chip 2014, 14, 3093.
- [32] T. Pan, D. Lu, H. Xin, B. Li, Light: Sci. Appl. 2021, 10, 124.
- [33] Y.-C. Chen, Q. Chen, X. Fan, Optica 2016, 3, 809.
- [34] F. Vollmer, S. Arnold, Nat. Methods 2008, 5, 591.
- [35] H. Lee, S. Michielsen, J. Text. Inst. 2006, 97, 455.
- [36] C. Neinhuis, W. Barthlott, Ann. Bot. 1997, 79, 667.
- [37] W. Wang, K. Lockwood, L. M. Boyd, M. D. Davidson, S. Movafaghi, H. Vahabi, S. R. Khetani, A. K. Kota, ACS Appl. Mater. Interfaces 2016,
- [38] D. Richter, M. Marinčič, M. Humar, Lab Chip 2020, 20, 734.
- [39] A. Kavčič, M. Garvas, M. Marinčič, K. Unger, A. M. Coclite, B. Majaron, M. Humar, Nat. Commun. 2022, 13, 1269.
- [40] A. H. Fikouras, M. Schubert, M. Karl, J. D. Kumar, S. J. Powis, A. Di Falco, M. C. Gather, Nat. Commun. 2018, 9, 4817.
- J. D. Eversole, H.-B. Lin, A. Huston, A. J. Campillo, P. T. Leung, S. Liu, K. Young, JOSA B 1993, 10, 1955.
- [42] N. A. Merabet, L. Cherbi, I. Haddouche, M. Benlacheheb, J. Yu, J. Opt. **2023**, 52, 1047.
- [43] N. Bhattarai, J. Gunn, M. Zhang, Adv. Drug Deliv. Rev. 2010, 62, 83.

ADVANCED OPTICAL MATERIALS

www.advancedsciencenews.com

www.advopticalmat.de

- [44] D. R. Rohindra, A. V. Nand, J. R. Khurma, South Pac. J. Nat. Appl. Sci. 2004, 22, 32.
- [45] A. Poghossian, H. Geissler, M. J. Schöning, Biosens. Bioelectron. 2019, 140, 111272.
- [46] G. Knothe, R. O. Dunn, J. Am. Oil Chem.' Soc. 2009, 86, 843.
- [47] M. Lu, S. S. Choi, U. Irfan, B. Cunningham, Appl. Phys. Lett. 2008, 93, 11.
- [48] E. Heydari, J. Buller, E. Wischerhoff, A. Laschewsky, S. Döring, J. Stumpe, Adv. Opt. Mater. 2014, 2, 137.
- [49] M. Karl, J. M. Glackin, M. Schubert, N. M. Kronenberg, G. A. Turnbull, I. D. Samuel, M. C. Gather, *Nat. Commun.* 2018, 9, 1525
- [50] H. T. Pham, J. Yoo, M. VandenBerg, M. A. Muyskens, J. Fluoresc. 2020, 30, 71.
- [51] K. Nawara, J. Waluk, Anal. Chem. 2019, 91, 5389.

- [52] Q. Chen, M. Ritt, S. Sivaramakrishnan, Y. Sun, X. Fan, Lab Chip 2014, 14, 4590.
- [53] H. A. Richards, C.-T. Han, R. G. Hopkins, M. L. Failla, W. W. Ward, C. N. Stewart Jr, J. Nutr. 2003, 133, 1909.
- [54] D. Lee, S. N. Beesabathuni, A. Q. Shen, Biomicrofluidics 2015, 9, 6.
- [55] J. H. Kim, T. Y. Jeon, T. M. Choi, T. S. Shim, S.-H. Kim, S.-M. Yang, Langmuir 2014, 30, 1473.
- [56] P. P. Ghimire, M. Jaroniec, J. Colloid Interface Sci. 2021, 584, 838.
- [57] EFSA ANS Panel, M. Younes, P. Aggett, F. Aguilar, R. Crebelli, B. Dusemund, M. Filipič, M. J. Frutos, P. Galtier, D. Gott, U. Gundert-Remy, G. G. Kuhnle, J.-C. Leblanc, I. T. Lillegaard, P. Moldeus, A. Mortensen, A. Oskarsson, I. Stankovic, I. Waalkens-Berendsen, R. A. Woutersen, M. Wright, P. Boon, D. Chrysafidis, R. Gürtler, P. Mosesso, D. Parent-Massin, P. Tobback, N. Kovalkovicova, A. M. Rincon, A. Tard, C. Lambré, EFSA J. 2018, 16, e05088.